The Effect of Ambient Air Condition on Heat Transfer of Hot Steel Plate Cooled by an Impinging Water Jet

Pil-Jong Lee*, Hae-Won Choi
Research Institute of Industrial Science and Technology (RIST), Pohang 790-600, Korea
Sung-Hong Lee
School of Mechanical Engineering, Pusan National University, Pusan 609-735, Korea

It has been observed that the cooling capacity of an impinging water jet is affected by the seasonal conditions in large-scale steel manufacturing processes. To confirm this phenomenon, cooling experiments utilizing a hot steel plate cooled by a laminar jet were conducted for two initial ambient air temperatures (10℃ and 40℃) in a closed chamber, performing an inverse heat conduction method for quantitative comparison. This study reveals that the cooling capacity at an air temperature of 10℃ is lower than the heat extracted at 40℃. The amount of total extracted heat at 10℃ is 15% less than at 40℃. These results indicate the quantity of water vapor, absorbed until saturation, affects the mechanism of boiling heat transfer.

Key Words : Impinging Liquid Jet, Hot Steel Plate, Ambient Air Temperature, Inverse Heat Conduction, Humidity Ratio

1. Introduction

Many industrial applications use free impinging jets since a high heat transfer rate can be obtained with relatively simple equipment. Impinging circular water jets are used in general as a rapid cooling system for hot steel plate. The high heat transfer rate by an impinging jet is caused by the high momentum, which can suppress the formation of a vapor film between the steel plate and fresh water. Previous studies indicate that cooling by impinging jets is more efficient by 10-30% than cooling by high-pressure spray jets (Roberts, 1983 ; Tracke et al. 1985).

Many researchers have studied the effect of variables on heat transfer such as impinging jet velocity, shape and size of the nozzle, the distance between the nozzle and the plate, the speed of moving plate, water temperature, and surface roughness. However, researches have been carried out mostly on single-phase convective cooling, and limited to nucleate boiling (Ruch et al., 1975 ; Katsuta et al., 1981 ; Lee et al., 1988 ; Vader et al., 1992). Only a few researchers have studied the heat transfer at high surface temperature with transition boiling and stable film boiling over Leidenfrost temperature (Ishigai et al., 1978 ; Kokado et al., 1984 ; Hatta et al., 1984 ; Oh et al., 1992).

Ishigai et al. (1978) examined the effect of sub-cooling and jet velocity on the steady state heat flux at the impinging point by two dimensional impinging liquid jet cooling in the range of 10-1000℃ of superheat. In a study of the cooling process with a hot steel plate by a circular impinging jet, Kokado et al. (1984) observed the effect of degree of sub-cooling or superheat temperature on the surface wetting. Hatta et al. (1984) have conducted similar unsteady cooling experiments and found that the radius of a single-phase convective cooling area is expanded in proportion to the square root of time. They also define the water-cooling area, including convective cooling

* Corresponding Author.
E-mail : leepj@rist.re.kr
TEL : +82-54-279-6636; **FAX** : +82-54-279-6888
Research Institute of Industrial Science and Technology (RIST), Pohang 790-600, Korea. (Manuscript **Received** April 13, 2002; **Revised** January 25, 2003)

and nucleate boiling, and determine the average heat transfer coefficient in this area. More recently, Oh et al. (1992) examined the effect of the initial surface temperature and the distance from nozzle to hot steel plate on the cooling rate.

We have recently discovered that the water flow rate to cool a hot steel plate of the same steel grade and size in steel making process is reduced by 20-30% in summer in comparison with that in winter, even if other operating conditions including water temperature are kept constant. Figure 1 shows the normalized heat flux variation, which is obtained from an in-line temperature control model for one specific steel grade and size group in a year. Although water temperature was maintained between 29-32℃ throughout the year, the heat flux between March and June is much higher than that between October and February.

In the examination on the effect of ambient air condition, which is the only one previous work, Filipovic et al. (1994) have quantified the contribution of impinging jet boiling, conduction through table roller, and air cooling including radiation heat transfer in strip cooling of the hot strip mill. They define radiation to ambient air to be a unique contribution to total heat transfer. However, if that were true, there could be no reason for the increased flow rate of cooling water in summer. We have theorized that ambient air temperature and humidity have an effect on heat transfer because of boiling in the thin liquid flow formed after jet impinging. No previous work has fully accounted for this phenomenon.

In this research, we confirmed the effect of ambient air condition on a hot steel plate cooled by an impinging water jet. To do this, we conducted cooling experiments for two different ambient air conditions and inverse heat transfer analyses. We suggest that the quantity of water vapor absorbed until saturation affects the mechanism of boiling heat transfer.

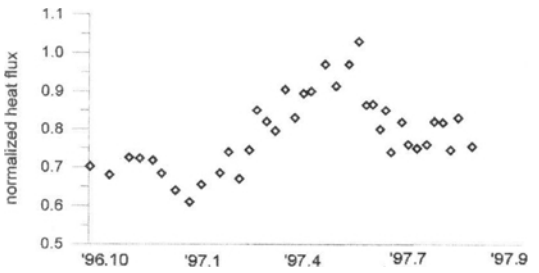

Fig. 1 Variation of normalized heat flux in a year

2. Experiments and Data Reduction

2.1 Experimental apparatus

A schematic diagram of the experimental apparatus is shown in Fig. 2. Cooling water is pumped into the cooling header for stabilizing the water flow and pressure from the large-scale storage tank and then discharged through the nozzle to the steel plate. Water temperature was controlled to 5−50℃ with an error range of ±0.2℃.

A chamber was fabricated with the size of 1 m ×1 m×1 m. Air in the chamber is heated or cooled to simulate summer and winter conditions. These temperature changes altered the initial relative humidity. The range of air temperature control is also 5−50℃ with an error range of ±0.2℃. Glass plates were installed on the front and back of the air chamber for easier visualization while other sides were covered with stainless 304 plates. To assist the evacuation of water vapor generated during cooling, two small fans were installed on the top of the air chamber.

An equipment with two guide rails and a stopper plate was set up to transport the hot

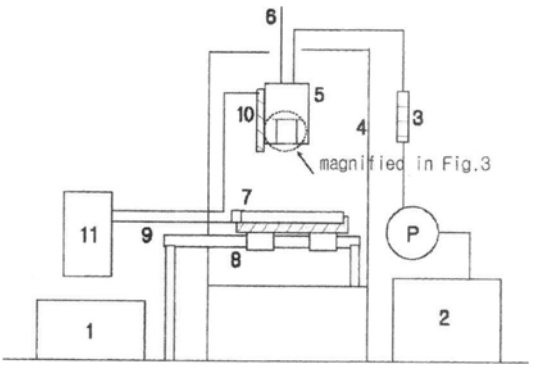

1. electric turnace 2. water reservoir 3. float flow meter 4. air chamber 5. water cooling header 6. air line 7. test specimen 8. transport equipment 9. thermocouples 10. transmitter for RH and temp. of air 11. data acquisition system

Fig. 2 Schematic diagram of experimental apparatus

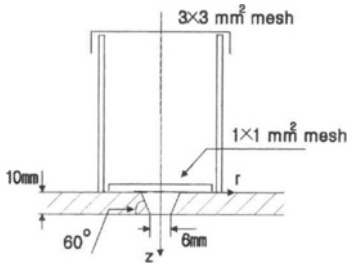

Fig. 3 Geometry of the convergent nozzle

specimen from outside the air chamber to the target cooling position inside the air chamber by keeping the horizontal level. The contacted width between the ceramic floor of the transport equipment and the test specimen was minimized to 5 mm to reduce the contact heat loss. In contrast to previous researches by Hatta et al. (1984) and Oh et al. (1992) who used a pipe nozzle, a convergent nozzle with 6 mm in outer diameter, as shown in Fig. 3, was adopted. This produced a uniformly thin film after impinging. To make the flow stable and laminar, a small cooling header with air vent was designed, where wire meshes were installed on the topside of the nozzle. The distance from nozzle to steel plate was fixed to 300 mm. Two valves were installed. One is for flow rate control and the other is for on/off control. A buoyant flow meter with a tolerance of ± 10 ml/min was used.

The specimen was made of stainless 304 with an as-rolled surface condition to avoid to the effect of oxide scale and phase transformation in the microstructure. We chose a smaller specimen with the size of 200 mm×200 mm×10 mm than Hatta et al. (1984) and Oh et al. (1992) to prevent thermal deformation during cooling process.

To measure the temperature change of the specimens, three K-type sheathed thermocouples with an outer diameter of 1.5 mm and 0.076 mm diameter alumina and cromel wires were installed on the bottom of the specimen at 0 mm ($x/d=0$), 30 mm ($x/d=5$) and 60 mm ($x/d=10$) in the radial direction from the impinging point. The alumina and cromel wires were stripped and spot-welded to the specimen. A T-type thermocouple with an outer diameter of 0.5 mm was set on the spout attached to the transport equipment. This measured the thermal history of the cooling water after impinging the specimen during the cooling process. Two OMAGA HX13V sensors for measuring the ambient air temperature and humidity were attached near the cooling header and the outer section of the air chamber. For visualization, a Nicon FM2 steel camera and Super VHS video camera were used.

2.2 Experimental methods

As a first step, the water was supplied to the cooling header when the targets for air temperature in the air chamber and water temperature in the water storage tank were obtained. To minimize deviations from the target water temperature, it is important to supply water to the cooling header just before cooling starts since its temperature cannot be controlled. As air ventilated from the water chamber and the control valve established the target water flow rate, the only on/off valve was turned off to confirm the target flow rate from the cooling start.

Before the experiments, the surface of the specimen was cleaned with ethanol and the thermocouples were attached. The specimen was heated to 940 ℃ in a muffle furnace and equalized by heating for more than 30 minutes at that temperature. After reaching a temperature of 800℃, the heated specimen was inserted into the air chamber. This delay in insertion was to prevent elevation of the air temperature inside the air chamber. When the specimen temperature reached 750℃, the on/off water valve was opened and cooling started. During cooling process, the air conditioner was turned off and small fans were turned on to sustain the natural flow of the water vapor generated by boiling.

2.3 Experimental conditions

For comparative analysis, two different air temperatures, 10℃ ±0.2℃ and 40℃ ±0.2℃ were selected for the air chamber, while the water temperature was kept constant at 40±0.2℃. Thus "W40A40" means the water and air temperatures were both 40℃. "W40A10" means a water temperature of 40℃ and an air temperature of 10℃.

We had two test sets with different water flow

rate and surface roughness conditions. In the first test set, the experiments for two different conditions of air temperature were conducted for water flow of 2090 ml/min ±10 ml/min over a specimen with an average surface roughness of 14.7 μm. These experiments were undertaken between 11 : 00 A.M. and 3 P.M. in one day to ensure a similar outer air condition. However, the constant outer air condition was not guaranteed. Therefore, in the second test set, we monitored the outer air condition and found it was kept constant at air temperature of 25℃ and relative humidity of 65% during the entire cooling process. To make the effect of ambient air temperature in the air chamber more clearly apparent by enhancing the boiling heat transfer, we increased the water flow rate to 3000 ml/min. The average surface roughness was 28 μm, which is two times larger than that of the 1st test set.

2.4 Data reduction

In contrast to previous works (Kokado et al., 1984; Hatta et al., 1984; Oh. et al., 1992), we tried to define the heat transfer characteristics by using the inverse heat conduction technique, not just cooling rate. An inverse heat conduction package developed by Trujillo at Trucomp Co. that use a regularization method was used to calculate the heat flux on the impinging surface from the measured hot plate temperatures.

Table 1 shows the thermo-physical properties (Kim et al., 1990) for this calculation, which are dependent on the temperature of the specimen. This situation was defined as an axi-symmetric, two-dimensional problem. The initial conditions were assumed to be a uniform 940 ℃. The adiabatic boundary conditions were applied to the surfaces, the side edge and the bottom except for the impingement side, since the radiation and convection heat transfer quantities on those are much less than the boiling heat transfer quantity on the impinging side. The calculation domain is shown in Fig. 4. Only three calculating regions for the unknown heat flux are defined since only three point-temperatures were measured.

Table 1 Thermo-physical property

$T(K)$	Cp(J/KgK)	ρ(kg/m³)	K(W/mK)
293	543.7	8000	17.09
680	697.1	8000	26.90
878	748.5	8000	31.29
973	757.3	8000	33.01
1072	761.0	8000	34.01
1158	781.6	8000	35.91

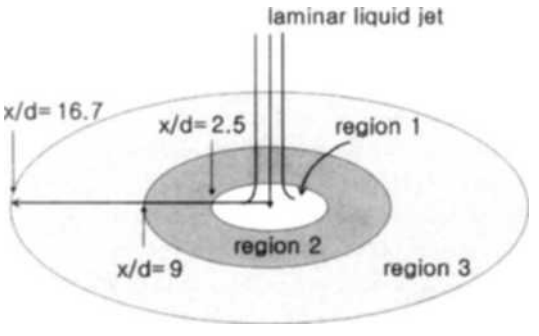

Fig. 4 Regions for calculating heat flux

3. Results and Discussion

3.1 Temperature history

Figure 5 compares the temperature history of the hot steel plate for two different conditions (W40A40 and W40A10) in the 1st test set. The temperatures were dropped dramatically after specific time delays. The order was $x/d=0$, $x/d=5$, and $x/d=10$ and the time delay between $x/d=0$ and $x/d=5$ was much less than that between $x/d=5$ and $x/d=10$. According to previous research results and data presented in this paper, the single-phase convective cooling area expanded as time went by and a strip of nucleate boiling developed at the boundaries of this area. The time delay and the difference between time delays could be explained by expansion of this area and the gradually reduced expansion rate. There was no significant difference between the measured temperatures in W40A40 condition and that in W40A10 condition under the impinging point ($x/d=0$). However, at the $x/d=5$ and $x/d=10$ positions, it was observed that at W40A40, the specimen cooled down more rapidly than at W40A10. This difference became more profound

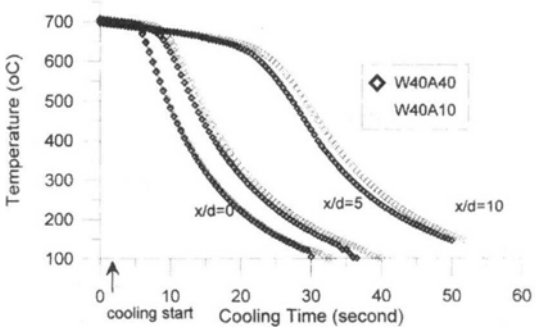

Fig. 5 Temperature history of the specimen (1st test set)

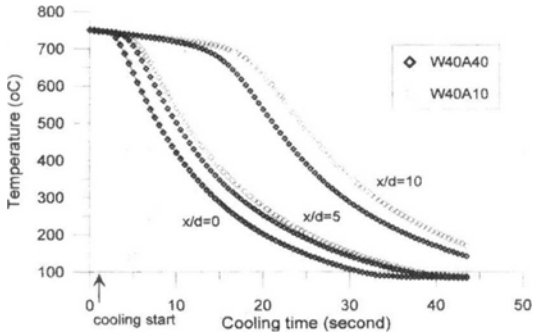

Fig. 6 Temperature history of the specimen (2nd test set)

as the x/d became larger.

Similarly, as shown in Fig. 6 for the 2nd test set, it was found that W40A40 caused more rapid cooling than W40A10. In this case, the difference between the two conditions (W40A40 and W40-A10) was larger than that in the 1st test set. This could be explained by the increased flow rate and rougher surface in the 2nd test set.

Figure 7 displays the measured water temperature obtained from a T-type thermocouple on the spout attached to the traversing equipment, which is used to gather the water that has flowed down from the steel plate. Just after cooling was initiated, the water temperature increased to 78℃. Thereafter, in the W40A40 condition, it maintained a temperature of about 70℃, which was approximately 10℃ higher than that of W40A10. Since the water temperatures of the jet were identical for both conditions, we inferred that the higher temperature of the flowed water was the result of heat transferred from the hot steel plate

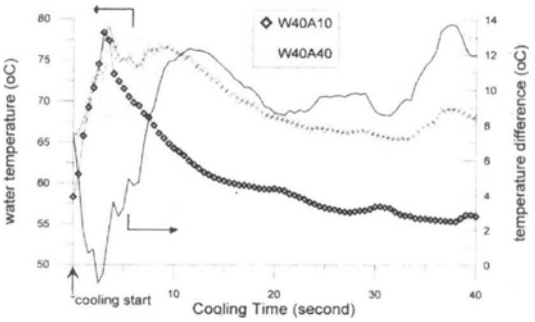

Fig. 7 Temperature history of the cooling water from the spout attached to traversing equipment (1st test set)

to the water. Our results demonstrated that the W40A40 condition allowed more active cooling than W40A10.

3.2 Monitoring the cooling process

The photographs of the successive stages during the cooling process are shown in Fig. 8 for the W40A40 condition and in Fig. 9 for the W40A10 condition. As cooling started, a water vapor film with a small white circular area suddenly formed near the impingement center and immediately disappeared. Then a single-phase convective cooling area, which was defined as "black zone" by Kokado et al. (1984), was developed and nucleate boiling was observed at the boundary of this area. However, the major part of the cooling surface still remained in the film boiling or radiation heat transfer. Also, an intense sputtering of small water droplets was observed near the boundary of the single-phase convective cooling area. It is speculated that this sputtering phenomenon results from flow boiling because the thin liquid film flow in the non-boiling case shows a hydraulic jump without sputtering, and also because the intensity of the sputtering weakened as the intensity of the boiling decreased.

As the cooling process proceeded, the radius of the single-phase convective cooling the area increased, but the rate of increase was reduced. Fig. 10 shows the change of this radius for the 1st and 2nd test set during the cooling process, as determined from video images. Similar to the results obtained by Hatta et al. (1984) and Oh. et

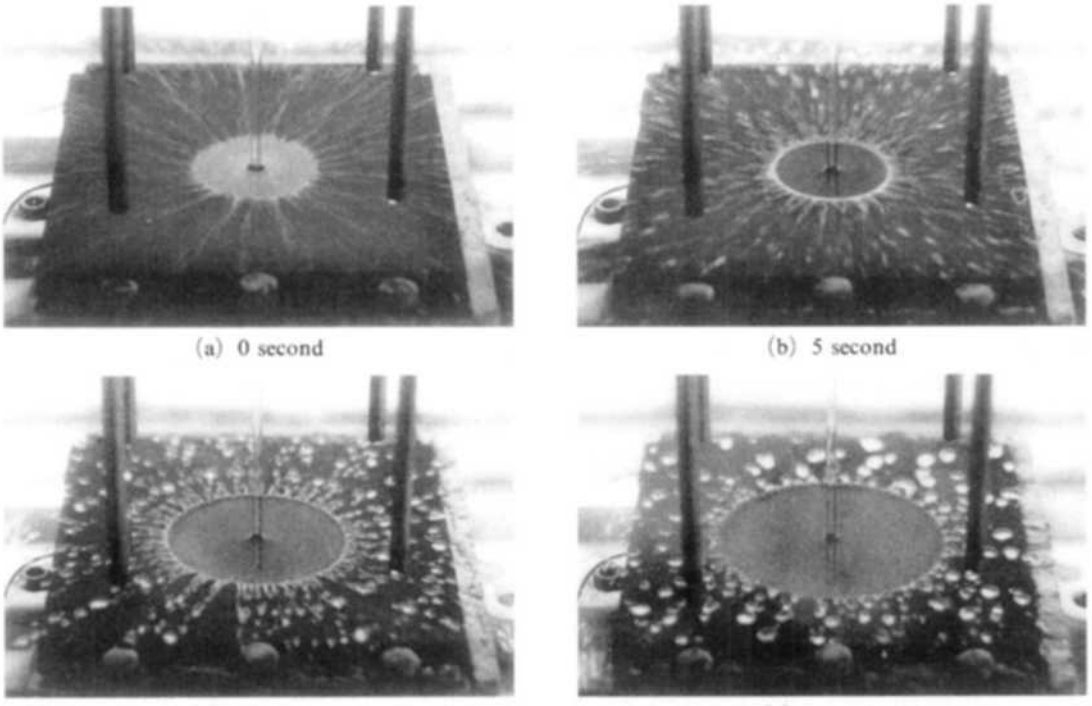

(a) 0 second (b) 5 second

(c) 15 second (d) 25 second

Fig. 8 Photographs of the successive stages for the cooling process (W40A40 condition, 2nd test set)

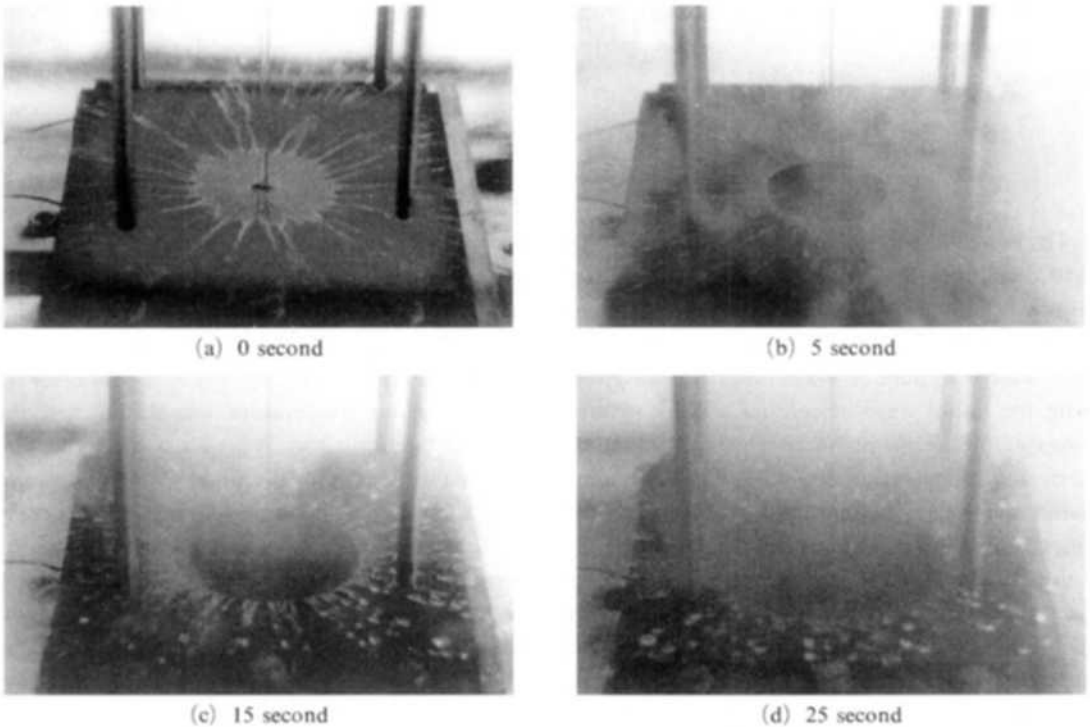

(a) 0 second (b) 5 second

(c) 15 second (d) 25 second

Fig. 9 Photographs of the successive stages for the cooling process (W40A10 condition, 2nd test set)

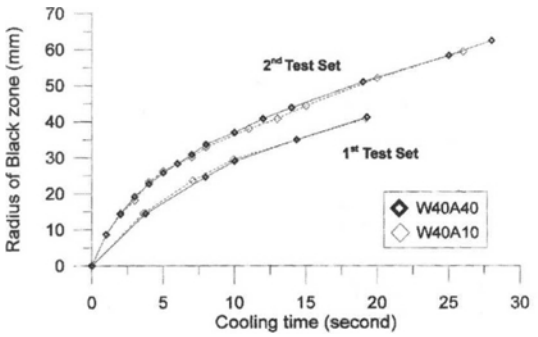

Fig. 10 Radius of single-phase convective cooling area (black zone) during the cooling process

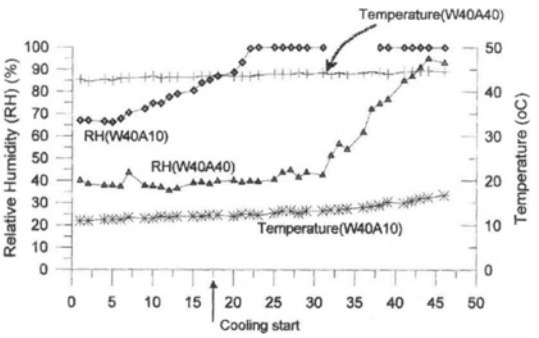

Fig. 11 Variations of the ambient air temperature and relative humidity during the cooling process

al. (1992), the expansion rates are proportional to the square root of the elapsed time. Equation (1) and (2) show the relationships between the radius and the elapsed time for each test set. The radius for the 2nd test set using a larger flow rate of 3000 ml/min and a rougher surface of 28 μm is larger than that for 1st test set using a smaller flow rate of 2090 ml/min and a less rough surface of 14 μm. However, there is no significant difference between the W40A40 and W40A10 conditions. It led us to conclude that this expansion rate could not be an important factor for estimating the cooling capacity, which differs from the opinion presented by Hatta et al. (1984).

$$R_{1st}=9.5\sqrt{t} \quad (1)$$

$$R_{2nd}=12.1\sqrt{t} \quad (2)$$

The two differences between W40A40 and W40-A10 conditions are demonstrated in Fig. 8 and Fig. 9. Firstly, in W40A10, with a lower air temperature that was contrary to the W40A40 condition, a large amount of water vapor was observed from the initial stage of cooling at the surroundings of the single-phase convective cooling or nucleate boiling areas. Secondly, when we compared the images taken at 5 seconds and 15 seconds for both conditions, in the W40A40 condition, the somewhat white area resulted from nucleate boiling and film boiling was clearer than that in the W40A10 condition. Between these two differences, the second one might mean that the intensity or area of boiling in the W40A40 condition is more active or wider than that in the W40A10 condition, which matches well with the previously mentioned results on the temperature history comparison.

On the contrary, the first difference might cause a misunderstanding that, due to the higher cooling capacity in the W40A10 condition, the amount of water boiled is larger than that in the W40A40 condition. Therefore, we monitored the air temperature and the relative humidity for the two different conditions in the 2nd test set (Fig. 11). The air temperature and relative humidity for the outside air was maintained at 25℃ and 65% during the cooling process. However heating up or cooling down of the inside air to the targeted 10℃ and 40℃ changed the relative humidity. Moreover the issued water for controlling the target flow rate without hot specimen and heating up of the air temperature by the hot specimen before cooling start changed the humidity ratio once again. Eventually, when cooling was initiated for the 10℃ target, the air temperature was 12.5℃ and the relativity humidity was 91%. For the 40℃ target, the air temperature was 43.5℃ and the relative humidity was 39%. We conjectured that the first difference for the water vapor (as seen in Fig. 8 and Fig. 9) might mean only the time delay until saturation rather than the cooling capacity. Actually, Fig. 11 shows that, while the W40A10 condition could be easily saturated in 5 seconds, the W40A40 condition was saturated nearly at the end of the cooling. Then, by reviewing the psychrometry chart that shows the relationships between the air temperature and the humidity ratio,

and the relative humidity in 1 kg of air, we found that about 0.01 kg of water vapor is required to reach saturation in the W40A10 condition, while more than 0.1 kg is needed in the W40A40 condition. This is more than 10 times the amount of water vapor as found in the W40A10 condition (Stoecker and Jones, 1982). So it was inferred that the previously mentioned large amount of water vapor observed in the W40A10 condition emerged because it could absorb only a small amount of water vapor until saturation, not because it has a high cooling capacity.

3.3 Comparisons of extracted heat

Numerical analysis using inverse heat conduction software was conducted for the two conditions of the 1st and 2nd test sets. Figure 12 compares the measured and calculated temperature histories for the W40A40 condition in the 1st test set. The differences between the measured and calculated temperatures were within 20℃ for all calculations.

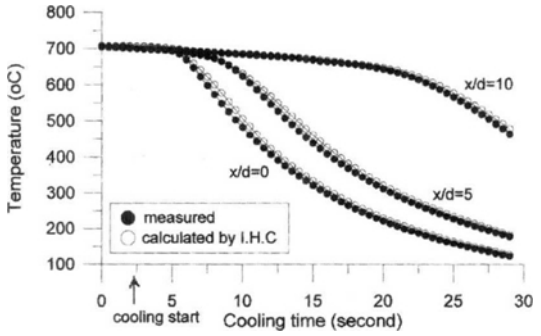

Fig. 12 Comparison between measured and calculated temperature (W40A40, 1st test set)

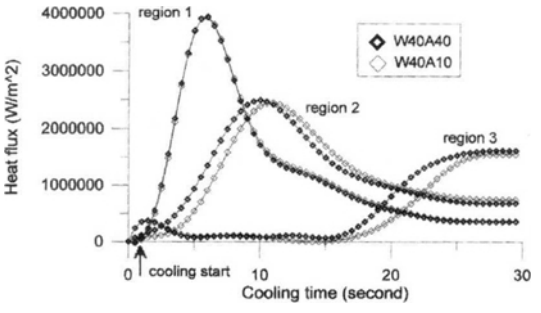

Fig. 13 Calculated heat fluxes during the cooling process (1st test set)

Figure 13 shows the histories of the calculated heat fluxes for the three regions shown in Fig. 4 in the 1st test set. At the start of cooling, the radiation or film boiling was dominant on all the regions. After that, as the single-phase convective heat transfer area expanded, each region experienced transition and nucleate boiling, and finally the single-phase convective heat transfer with time delay between each one. This is why the calculated heat fluxes stayed in low values in radiation or film boiling and increased to the maximum at nucleate boiling, and thereafter decreased experiencing the single-phase convective cooling. Among the three regions of Fig. 4, the maximum heat flux appeared on the region closest to the impinging point, as we had expected. Between the two different conditions, there is no significant difference on the region closest to the impinging point for the entire cooling process. But, on the other two regions, the heat flux before the maximum value in the W40A40 condition is larger than that in the W40A10 condition except for the initial radiation and final single-phase convective cooling.

To quantify the difference in the heat transfer between the two different air conditions, the amount of the total extracted heat was compared. The amount of total extracted heat for 27 seconds from cooling start was calculated by integrating the data in Fig. 13 with respect to time, multiplying the area of the heat transfer region, and summing up all values for three regions. This time, 27 seconds was selected because it meant that the region farthest from the impinging point was going into single-phase convective cooling for the two different air conditions. Table 2 compares the total heat flows between the two air conditions in the 1st and 2nd test sets. As had been expected, the amount of the extracted heat in the 1st test set was smaller than that in the 2nd test set. In the both test sets, it was discovered that the amount of total extracted heat in the case of 10℃ was smaller by nearly 15% than that of the 40℃ condition.

Results of uncertainty analysis for the measurements of major variables, which effect on the amount of the extracted heat during the cooling process, are tabulated in Table 3. The cooling

Table 2 Comparison of extracted heat between W40A10 and W40A40 conditions

Condition / Case	W40A40, ①, (10^6 J)	W40A10, ②, (10^6 J)	Deviation, (①-②) * 100/②, (%)
1st test set	6.47	5.61	15.3
2nd test set	9.11	7.84	16.2

Table 3 Uncertainty in measurements

Variable	Uncertainty (%)
Ambient air temperature	2.14
Position of thermocouple	3.33
Water temperature	0.91
Time	0.93
Specimen temperature	0.76
Water flow rate	0.33

surface of the specimen was cleaned by alcohol when it was prepared and its horizontal level and the position were frequently checked. Also a specimen was used for a experiment to prevent the error by its deformation. Therefore we thought that the errors by the surface condition and the position of the test specimen were negligible.

For the uncertainty analysis of the total extracted heat, the method of single sample experiments proposed by Kline and McClintock (1953) was selected. It was assumed that the total extracted heat is directly or inversely proportional to the variables listed in Table 3. The uncertainty of the total extracted heat in the W40A10 condition was estimated as 4.25%.

3.4 Relation between normalized heat flux and Δ water vapor quantity

In the comparison of extracted heat above, it was found that the transferred heat in the easily saturated W40A10 condition was smaller than that in the W40A10 condition, which could absorb much amount of water vapor until saturation. Other variables such as liquid flow rate, liquid temperature, nozzle shape, and distance between specimen and nozzle remained the same. According to these results, it is reasoned that, for

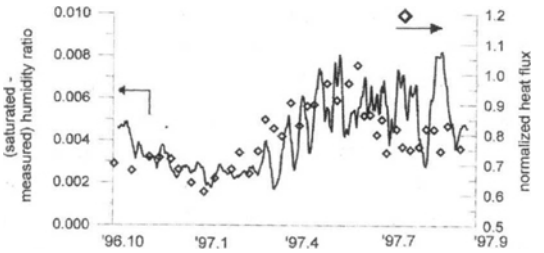

Fig. 14 Variations of the normalized heat flux and Δ water vapor quantity in a year

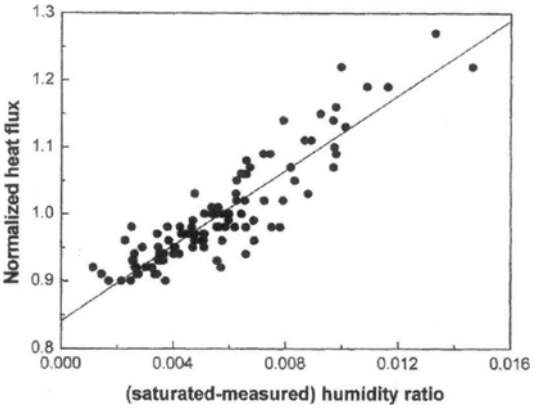

Fig. 15 Comparison between normalized heat flux and Δ water vapor quantity (Mild Steel, thickness between 5-6 mm)

the exact comparison of the cooling capacity, it is necessary to account for how much water vapor could be absorbed in the ambient air.

Consequently, we have calculated Δ water vapor quantity of the ambient air by using local meteorological observations for a year (Fig. 1). Here Δ water vapor quantity is defined as the difference of the weight of water vapor in 1 kg of air determined from the measured ambient air temperature and the relative humidity with that in 1 kg of air at saturation state for the same ambient temperature. Figure 14 shows this calculated quantity with the normalized heat flux. As we observed, Δ water vapor quantity explains the transition of normalized heat flux very well. Figure 15 shows the relationship between the normalized heat flux and Δ water vapor quantity for different size and material specifications from those in Fig. 1. From these results, it is concluded that the Δ water vapor quantity may be one of the major

factors that govern the mass diffusion of water vapor into ambient air from a boiling system.

4. Conclusions

The experiments were conducted under two different ambient air temperatures-10℃ and 40℃ in a closed chamber to confirm the seasonal variation of the cooling capacity in the case of impinging jet cooling of a hot steel plate. The conclusions of this study can be summarized as follows :

(1) Heat transfer becomes more active in high ambient air temperature than that in the relatively low ambient air temperature when all other factors except for the humidity ratio remain constant.

(2) The developing rate of the single-phase convective heat transfer area is proportional to the square root of the elapsed time, but it is independent of the ambient air conditions.

(3) The ambient air condition affect the boiling phenomenon with a thin liquid film and the total heat transferred quantity at 10℃ ambient air temperature is smaller by nearly 15% than that at 40℃ .

(4) The quantity of water vapor absorbed until saturation, can accurately explain the seasonal transition of heat flux in impinging jet cooling process of hot steel plate. Consequently to improve the cooling control accuracy, it is necessary to consider Δ water vapor quantity.

Acknowledgment

The authors gratefully acknowledge the support of POSCO in carrying out this study.

References

Filipovic, J., Viskanta, R., Incropera, F. P. and Veslocki, T. A., 1994, "Cooling of a Moving Steel Strip by an Array of Round Jets," *Steel Research*, Vol. 65, No. 12, pp. 541～547.

Hatta, N., Kokado, J., Takuda, H., Harada, J. and Hiraku, K., 1984, "Predictable Modelling for Cooling Process of a Hot Steel Plate by a Laminar Water Bar," *Arch. Eisenhuttenwes*, Vol. 55, No. 4, pp. 143～148.

Ishigai, S., Nakanishi, S. and Ochi, T., 1978, "Boiling Heat Transfer for a Plane Water Jet Impinging on a Hot Surface," *Int. Heat Transfer Conf*., 6th, pp. 445～450.

Katsuta, M. and Kurose, T., 1981, "A Study on the Boiling Heat Transfer of Thin Liquid Film (Part 2, Nucleate Boiling Heat Flux, ," *JSME*, Vol. 47, No. 421, pp. 1849～1860.

Kim, S. J., 1990, *Characteristics of Thermo-Physical Properties of Various Kinds of Steel at Elevated Temperature*, Research Report, Research Institute of Industrial Science and Technology.

Kline, S. J. and McClintock, F. A., 1953, "Describing Uncertainties in Single-Sample Experiments," *Mechanical Engineering*, Vol. 75, pp. 3～8.

Kokado, J., Hatta, N., Takuda, H., Harada, J. and Yasuhira, N., 1984, "An Analysis of Film Boiling Phenomena of Subcooled Water Spreading Radially on a Hot Steel Plate," *Arch. Eisenhuttenwes*, Vol. 55, No. 3, pp. 113～118.

Lee, K. W. and Kim, Y., 1988, "A study on the Boiling Heat Flux on High Temperature Surface by Impinging Water Jet," *KSME*, Vol. 12, No. 1, pp. 81～94.

Oh, S. M. and Lee, S. J., 1992, "Cooling Chacterisrics of a Hot Steel Plate by a Circular Impinging Liquid Jet," *KSME*, Vol. 16, No. 6, pp. 1150～1155.

Roberts, W. L., 1983, *Hot Rolling of Steel*, Marcel Dekker, New York.

Ruch, M. A. and Holman, J. P., 1975, "Boiling Heat Transfer to a Freon-113 Jet Impinging Upward onto a Flat Heated Surface," *Int. J. Heat Mass Transfer*, Vol. 18, pp. 51～60.

Stoecker, W. F. and Jones, J. W., 1982, *Refrigeration and Air Conditioning*, McGraw-Hill, New York.

Tacke, G., Litzke, H. and Raquet, E., 1985, "Investigations into the Efficiency of Cooling Systems for Wide-Strip Hot Rolling Mills and Computer-Aided Control of Strip Cooling, in Accelerated Cooling of Steel," P. D. Southwick, Ed., *The Metallurgical Socity*, Warrendale Pa., pp. 35～54.

Trujillo, D. M., INTEMP user's manual, TRUCOMP CO., CA.

Vader, D. T., Incropera, F. P. and Viskanta, R., 1992, "Convective Nucleate Boiling on a Heated Surface Cooled by an Impinging, Planar Jet of Water," *J. Heat Transfer*, Vol. 114, pp. 152~160.